Journal of Molecular and Cellular Cardiology Plus 13 (2025) 100481

Contents lists available at ScienceDirect

Journal of Molecular and Cellular Cardiology Plus

journal homepage: www.journals.elsevier.com/journal-of-molecular-andcellular-cardiology-plus

Med13 and Med13L: Critical redundant players in basal cardiac function and gene expression

Kayla M. Henry [a,b], Richard N. Gardner [a], Alexis M. Oppman [a], Nastaran Daneshgar [a,c], Mariela Rosales [a], Ines Martins [a], Kedryn K. Baskin [d], Chad E. Grueter [a,b,*]

[a] Department of Internal Medicine, Division of Cardiovascular Medicine, Francois M. Abboud Cardiovascular Research Center, Fraternal Order of Eagles Diabetes Research Center, University of Iowa, Iowa City, IA, USA
[b] Interdisciplinary Graduate Program in Genetics, University of Iowa, Iowa City, IA, USA
[c] Department of Pathology, University of Iowa, Iowa City, IA, USA
[d] Department of Physiology and Cell Biology, Dorothy M. Davis Heart and Lung Research Institute, The Ohio State University Wexner Medical Center, Columbus, OH, USA

ARTICLE INFO

Keywords:
Med13
Med13L
Cardiac function
Heart failure
Mediator complex
Transcription

ABSTRACT

Background: Previous studies have linked mutations in the Mediator complex, specifically Mediator 13 (Med13) and Mediator 13-like (Med13L), with both congenital heart defects and cardiovascular diseases. Med13 and Med13L are mutually exclusive paralogs within the kinase submodule of the Mediator complex that have been shown to have partially redundant functions in embryonic development and transcription, but their combined roles have not been investigated in the adult heart. We investigated the critical yet redundant roles of Med13 and Med13L in adult murine cardiomyocytes for basal cardiac function.

Methods: We generated an inducible Med13 and Med13L cardiomyocyte-specific knockout mouse model to investigate Med13 and Med13L regulation of cardiac function and transcription. We performed RNAseq on mice four weeks after the start of tamoxifen to identify changes in gene expression. Differentially expressed genes were compared across cardiac knockouts of Med13/13L, Med13, Med12, Med1, and Med30 elucidating similar mechanisms of cardiac dysfunction.

Results: Med13/13L knockout resulted in decreased cardiac function leading to lethal heart failure in a median timeframe of 6 weeks from the start of tamoxifen. There is significant gene dysregulation after Med13/13L knockout with similar gene dysregulation of fibrotic pathways and calcium handling across Mediator cardiac knockouts.

Conclusions: Med13 and Med13L function partially redundantly within the heart to maintain basal cardiac function and transcription, as well as redundancies within cardiac phenotypes related to mediator complex disruptions.

1. Introduction

The heart undergoes dynamic changes in transcription, both during development and in response to cardiac stressors [1–3]. Changes in gene expression profiles in response to cardiac stressors or genetic modifications are integrated through signal-dependent transcription factors and the Mediator complex to modulate gene expression and activate the hypertrophic gene network [4–7]. The Mediator complex is a 1.2 kDa complex that interacts with RNA polymerase II and DNA-bound transcription factors to form the preinitiation complex [5,8]. Mediator is comprised of a head, middle, and tail region with roughly 26 subunits and a reversibly disassociating kinase submodule. The kinase submodule contains cyclin-dependent kinase 8 (CDK8), Cyclin C, Mediator 12 (MED12) and Mediator 13 (MED13) [8].

* Corresponding author at: University of Iowa, 4332 Pappajohn Biomedical Discovery Building (PBDB), Iowa City, IA 52242, USA.
E-mail address: chad-grueter@uiowa.edu (C.E. Grueter).

https://doi.org/10.1016/j.jmccpl.2025.100481
Received 14 April 2025; Received in revised form 13 August 2025; Accepted 23 August 2025
Available online 31 August 2025

Within the Mediator complex, Med13 has been shown to have a mutually exclusive paralog, Mediator 13-like (Med13L), which is conserved across vertebrate species and arose from a gene duplication [9,10]. Due to this conservation, it has been previously shown that MED13/13L have significant redundancy in the regulation of super-enhancer-associated genes within colon cancer cells [11]. Embryonic development in mice has shown that Med13 and Med13L can partially compensate for one another but still maintain independent functions [12]. Human mutations within MED13 or MED13L are associated with both congenital heart defects and cyanotic cardiovascular disease, as well as growth delays and intellectual disabilities [10,13–17]. Despite the conserved nature of MED13/13L in both redundant and independent functions, their roles within the heart are not fully understood.

We and others have demonstrated that cardiomyocyte-specific deletions of Med13, cyclin C and Med1 play a key role in regulating systemic energy along with mitochondrial and metabolism gene expression [18–25]. Similarly, overexpression of Cdk8 in cardiomyocytes causes sarcomeric and metabolic pathways dysregulation [26]. Furthermore, Med12, Med27, and Med30 have been shown to play crucial roles in maintaining cardiac function leading to dilated cardiomyopathy [27–29]. Overall, these findings demonstrate the crucial role of the Mediator complex in integrating transcriptional signals to orchestrate basal cardiac function which hasn't been explored in regard to Med13/13L redundancy.

Despite efforts to understand how the cardiac transcriptome changes in a disease state, the role of the Mediator complex and kinase submodule in heart failure is incompletely understood. We utilized an adult mouse model of cardiomyocyte-specific deletion of both Med13 and Med13L to investigate their redundant roles and effect on cardiac transcription and function. We also investigated the redundant regulatory function of the Mediator complex itself due to similar cardiac phenotypes across several Mediator subunit knockout mouse models to identify regulation of common cardiac gene networks.

2. Methods

2.1. Animal model

Med13 conditional knockout mice used in this study have been previously described [19]. The Med13L mouse strain used for this research project, C57BL/6 N-*Med13l*$^{tm1a(KOMP)Wtsi}$/MbpMmucd, RRID: MMRRC_048567-UCD, was obtained from the Mutant Mouse Resource and Research Center (MMRRC) at University of California at Davis, an NIH-funded strain repository, and was donated to the MMRRC by The KOMP Repository, University of California, Davis; Originating from Kent Lloyd, UC Davis Mouse Biology Program [30]. All animal procedures were approved by the University of Iowa Office of the Institutional Animal Care and Use Committee. Med13 and Med13L mice containing LoxP sites flanking exon 7/8 and exon 11 (Med13/13L fl/fl), respectively, were bred to Myh6-Mer-Cre-Mer mice (C57bl/6 background, Jackson Labs C56BL/6NJ stock No. 005304) to generate mice with a tamoxifen-inducible cardiomyocyte-specific deletion of Med13 and Med13L (Med13/13L dKO). Mice were housed under standard 12 h light/dark cycles. Med13/13L dKO mice and Med13/13L Cre-negative littermate mice were placed on either normal chow (NC) or tamoxifen (TAM) chow (40 mg·kg^{-1}·day^{-1}; Teklad diet, Harlan, Indianapolis, IN) for 2 weeks starting at 8 weeks of age. All experiments were performed on multiple distinct litters with multiple batches of tamoxifen to prevent batch effects. Experiments were performed on male mice with primary results validated in female mice.

2.2. Echocardiography

Cardiac function was assessed via high-frequency echocardiography (30 MHz) linear array transducer (Vevo 2100; Visual Sonics, Toronto, ON Canada). Parasternal long and short axis views were obtained in unsedated mice, and measurements were performed by a single experienced and blinded technician from the University of Iowa Cardiovascular Phenotyping Core.

2.3. Histology

Hearts were preserved in 4 % paraformaldehyde and embedded in paraffin. Sectioning (7 μm) and H&E staining was performed by the University of Iowa Central Microscopy Research Facility. Transverse sections of the ventricles were stained with hematoxylin and eosin for morphological analysis. Mason's trichrome staining (Epredia) was performed for quantification of fibrosis. Histology was performed on three to four hearts per group. Pictures were taken using a Keyence BZ-X810 Fluorescence microscope (Keyence, Osaka, Japan).

To quantify fibrosis, a blinded analyst took 6.25× magnification snapshots from Qupath and loaded into ImageJ. Areas chosen for analysis could not contain section overlapping, major blood vessels, and could not contain background. Using ImageJ, the snapshots were converted to an RGB stack and thresholded to an 81 lower limit, and 162 upper limit to quantify the level of stained collagen. This was analyzed by ImageJ and converted into a % area measurement. Each heart was analyzed in triplicate with the average % area for each heart being plotted.

2.4. RNA-sequencing

Flash-frozen, pulverized ventricles were used to extract RNA through a Monarch Total RNA miniprep kit (New England Biolabs, Ipswich, MA). RNA quality and integrity were assessed through Qubit analysis. The University of Iowa Institute of Human Genetics generated RNA libraries through a TruSeq Stranded Total RNA with RiboZero Gold kit (Illumina, San Diego, CA). RNA sequencing was performed on a Novaseq 6000 genome sequencing platform (Illumina), then analyzed using BaseSpace (Illumina). Raw sequences were aligned to UCSC mm10 using Bowtie2 v2.2.6. Alignments were uploaded into the Cufflinks Assembly and DE v2.1.0 (BaseSpace Workflow, Illumina). Differentially expressed genes were calculated based on a Log2FC $>$ 1.0 and q-value $<$0.05, then analyzed via Ingenuity Pathway Analysis (IPA; Qiagen, Hilden, Germany). Med13/13L dKO RNA-seq data can be found at GSE298801.

2.5. RNA-seq comparison

RNA-seq datasets were accessed as follows MED1 (GSE84160), MED12 (GSE100088), MED13 (GSE124117) and MED30 (GSE181534). Differentially expressed genes were classified according to previously published thresholds [18,25,27,28]. Differential gene overlap was quantified and plotted using Venny v2.1 [31]. Ingenuity Pathway Analysis (IPA) was performed on the differentially expressed genes for each condition. IPA for each condition was then compared within IPA to determine the activation z-score across groups.

2.6. qRT-PCR

To validate our RNAseq, we performed qRT-PCR using the Fast Sybr (Invitrogen) system and measured on a Quantstudio 3 (Applied Biosystems) All reactions were performed in triplicate normalized against 18S and calculated using the $2^{-\Delta\Delta CT}$ method. Primers used as follows.

Gene	Forward 5′-	Reverse 5′-
18S	GTAACCCGTTGAACCCCATT	CCATCCAATCGGTAGTAGCG
Acta1	CGACATCAGGAAGGACCTGTATGCC	AGCCTCGTCGTACTCCTGCTTGG
Col1a1	TCCGGCTCCTGCTCCTCTTA	GTATGCAGCTGACTTCAGGGATGT
Col3a1	GCCCACAGCCTTCTACAC	CCAGGGTCACCATTTCTC
Nppa	CCAGGCCATATTGGAGCAAA	GAAGCTGTTGCAGCCTAGTC
Nppb	GCTGCTTTGGGCACAAGATAG	GCAGCCAGGAGGTCTTCCTA
Tgfb1	AGAGGTCACCCGCGTGCTAA	TCCCGAATGTCTGACGTATTGA

2.7. PRALINE alignment

FASTA protein sequences were obtained from NCBI as follows: *Homo sapiens* MED13 (NP_005112.2), *Homo sapiens* MED13L (NP_056150.1), *Mus musculus* MED13 (NP_001074400.1), *Mus musculus* MED13L (NP_001334374.1). Domains were identified as follows: N-terminal (CDD:463303), PIWI (CDD:465699), C-terminal (CDD:461879). PRALINE was run using default PRALINE parameters: exchange weights matrix (BLOSUM62), associated gap penalties 12 open, 1 extension, PSI-BLAST pre-profile processing (homology-extended alignment), and PSI-BLAST iterations- 3 at *E*-value cutoff 0.01 [32].

2.8. Statistical analysis

Statistical significance was defined as $p < 0.05$ unless otherwise stated. Analyses were performed using GraphPad Prism v10.2.1. To determine statistical significance, a two-tailed unpaired Student's *t*-test was used to compare two groups while an ANOVA with Tukey post-hoc analysis was used to compare three or more groups. A log-rank test (Mantel-Cox) was performed for survival curve analysis. All data are expressed as mean ± standard error.

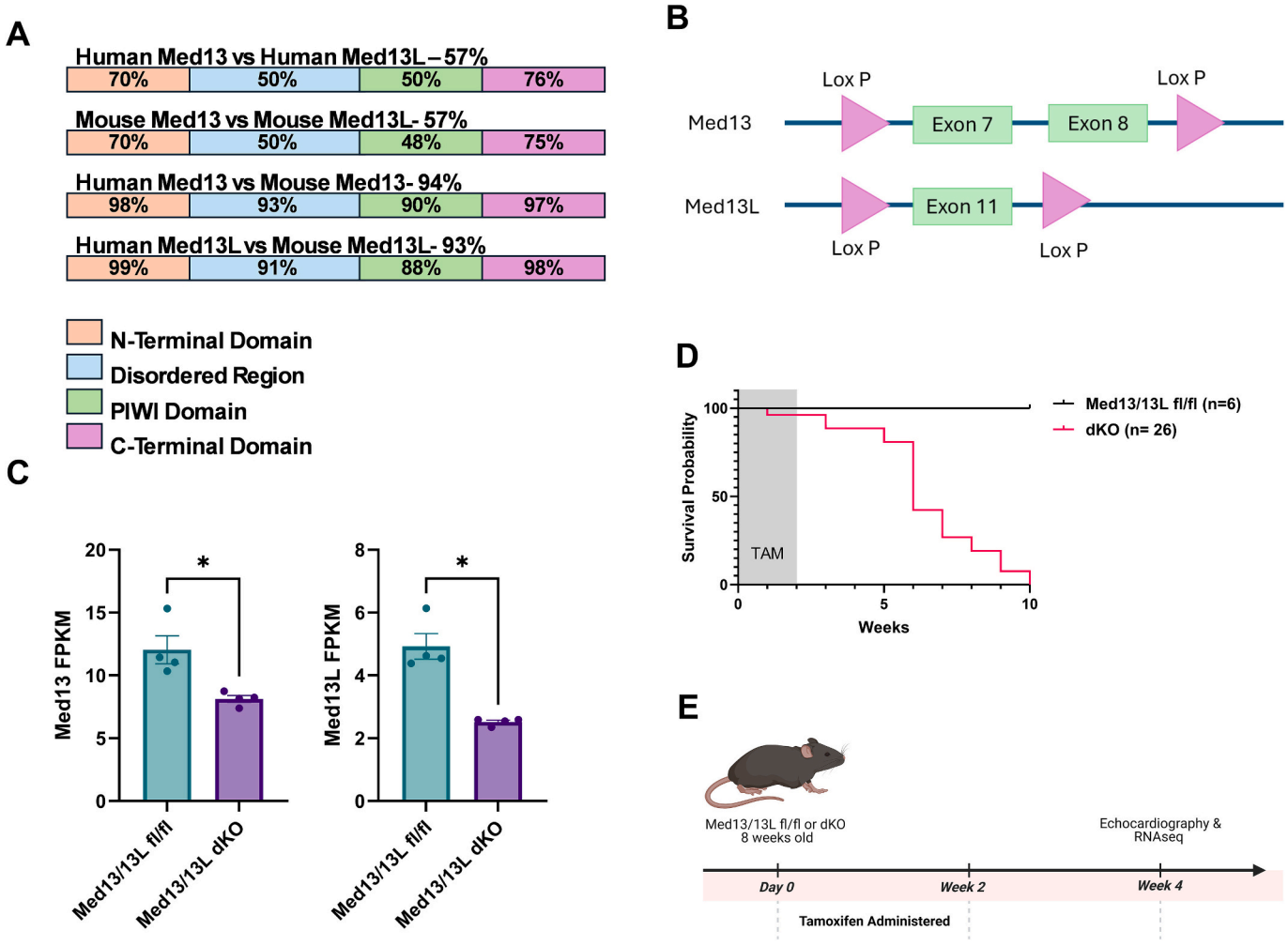

Fig. 1. Generation of Med13/13L double knockout mouse model A) PRALINE comparison of human and mouse isoforms of MED13 and MED13L. B) MED13/13L deletion. C) FPKM values for Med13 and Med13L in Med13/13L fl/fl (n = 4) and Med13/13L dKO (n = 4). *t*-test performed with significance as $p < 0.05$. Standard error bars are displayed. D) Kaplan-Meier survival curve of WT vs. MED13/13L dKO mice. WT, n = 6; dKO, n = 26. E) Mouse experimental timeline. Created using Biorender.

3. Results

3.1. Cardiac Med13 or Med13L is necessary for survival in adult mice

The homologous nature of Med13 and Med13L led us to investigate the domain sequence similarity between both human and mouse forms of Med13/13L. PRALINE alignments demonstrated 57 % sequence similarity between Med13 and Med13L in both species (Fig. 1A). Comparisons of hMed13/mMed13 and hMed13L/mMed13L each showed 94 % sequence similarity. The similarity between the species indicates a high level of conservation throughout mammalian evolution, as well as indicating that there might be a preserved function for maintaining basal homeostasis.

The critical role for Mediator complex proteins and the increased susceptibility of Med13 knockout mice to hypothyroidism led us to investigate whether Med13 and Med13L have redundant yet necessary roles in maintaining cardiac function. Deletion of Med13 and Med13L using αMHC Cre is embryonic lethal. Mendelian ratios were achieved at E15.5; however, at weaning, there were no double knockout mice observed (Med13 fl/fl /13L fl/fl αMHC-Cre +). Therefore, we generated a tamoxifen-inducible cardiomyocyte-specific deletion of Med13 and Med13L under a Myh6- MerCreMer promoter (Med13/13L dKO) (Fig. 1B). Tamoxifen chow was administered for 2 weeks starting at 8 weeks of age and FPKM values confirmed significant loss of Med13 and Med13L in Cre-positive mice compared to Cre-negative mice (Fig. 1C).

We then performed a survival analysis of Med13/13L dKO mice (n =

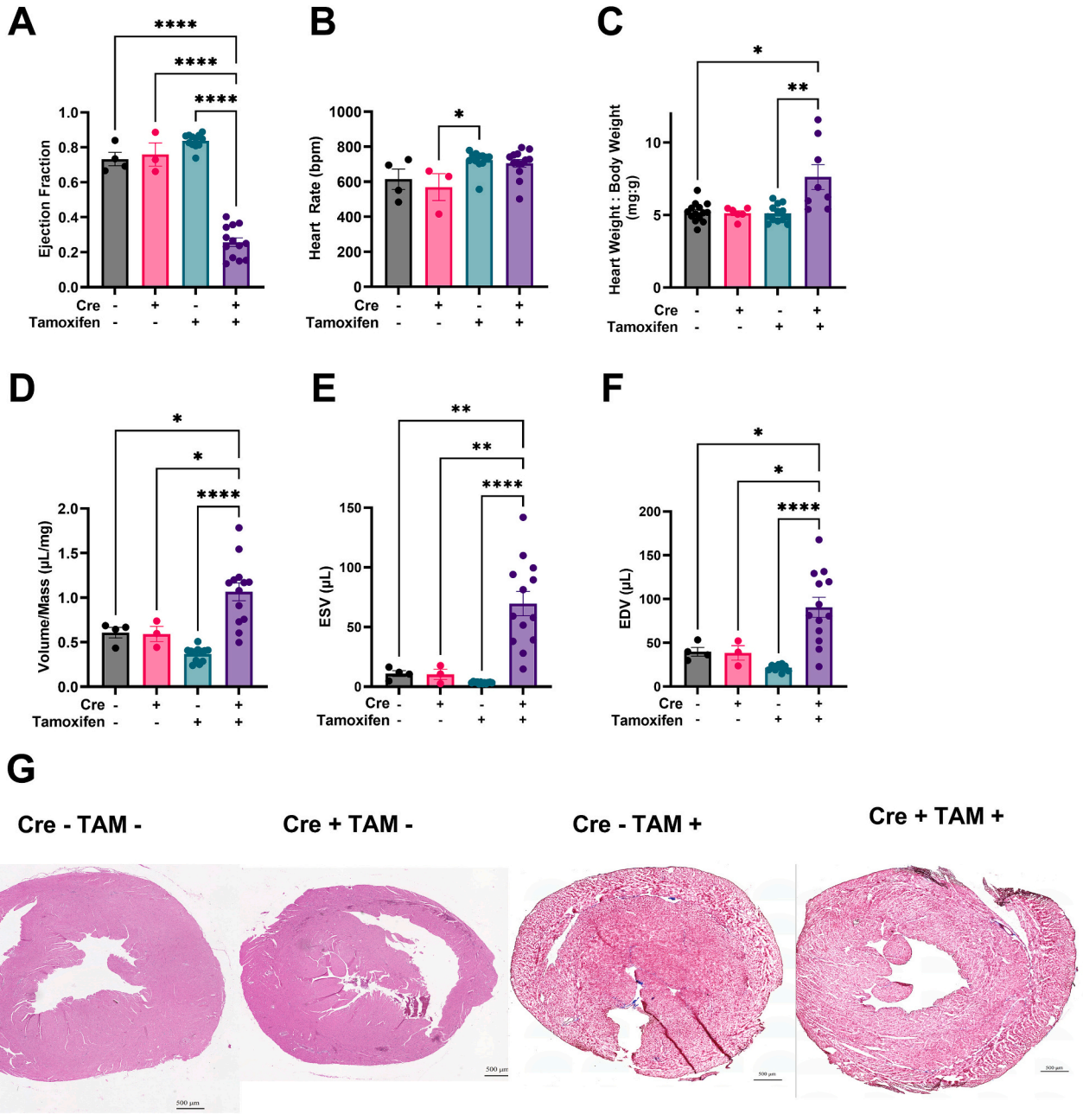

Fig. 2. Deletion of Med13 and Med13L causes lethal heart failure. Ordinary One Way ANOVA with Tukey's Multiple Comparisons performed with significance a $p < 0.05$. Standard error bars displayed. A) Ejection fraction at 4 weeks from start of tamoxifen chow. Cre -, TAM - (n = 4) Cre +,TAM - (n = 3), Cre -, TAM + (n = 12); Cre +, TAM + (n = 13). B) Heart weight:body weight ratio at 4 weeks from start of tamoxifen. Cre -, TAM - (n = 14); Cre +, TAM - (n = 6), Cre -, TAM + (n = 13); Cre +, TAM + (n = 8). C–F) Echocardiography data from mice at 4 weeks from start of tamoxifen. Cre -, TAM – (n = 4); Cre +,TAM – (n = 3), Cre -, TAM + (n = 12); Cre +, TAM + (n = 13). G) Representative H&E stains.

Table 1
Echocardiogram data.

Genotype	Cre	Tamoxifen	Sex	n	Body Weight	Heart Weight: Body Weight	Heart Weight	LV Thickness	Heart Rate	ENDOarea; d	ENDOarea; s	ENDOmajr; d	ENDOmajr; s	EPIarea;d	EPImajr; d	End Diastolic Volume	End Systolic Volume	Mass (mg)	Vol/ mass	SV mcL	CO mcL/m	Ejection Fraction
Med13/ 13L	+	+	M	13 (4)	23.44 ± 0.77	5.92 ± 0.35	138.1 ± 3.79	0.59 ± 0.017	702.26 ± 20.83	11.50 ± 1.78	8.43 ± 1.83	6.83 ± 0.25	6.14 ± 0.32	21.41 ± 2.089	7.64 ± 0.23	69.61 ± 12.80	48.79 ± 12.044	74.42 ± 5.046	0.86 ± 0.11	20.82 ± 1.85	14,432.64 ± 1208.98	0.44 ± 0.081
Med13/ 13L	+	−	M	3	22.96 ± 0.067	5.42 ± 0.048	124.53 ± 1.28	0.64 ± 0.008	569 ± 77.022	6.95 ± 1.45	2.16 ± 0.87	6.61 ± 0.11	5.56 ± 0.25	15.53 ± 1.85	7.62 ± 0.14	38.49 ± 8.24	10.34 ± 4.32	63.53 ± 5.076	0.59 ± 0.085	28.15 ± 3.92	15,900.75 ± 3008.73	0.75 ± 0.066
Med13/ 13L	−	+	M	12	23.37 ± 0.57	5.78 ± 0.56	133.25 ± 10.72	0.65 ± 0.035	716.38 ± 21.40	8.06 ± 1.64	4.91 ± 1.63	6.40 ± 0.25	5.30 ± 0.37	17.58 ± 1.84	7.31 ± 0.21	46.51 ± 11.83	26.94 ± 10.68	66.71 ± 4.041	0.64 ± 0.12	19.56 ± 1.87	13,781.17 ± 1164.68	0.60 ± 0.081
Med13/ 13L	−	−	M	4	23.34 ± 0.60	5.49 ± 0.12	128.15 ± 4.13	0.64 ± 0.019	594.71 ± 57.38	7.11 ± 0.99	2.27 ± 0.56	6.63 ± 0.097	5.54 ± 0.14	15.99 ± 1.37	7.57 ± 0.11	39.27 ± 5.42	10.70 ± 2.75	64.77 ± 4.29	0.60 ± 0.06	28.56 ± 2.85	16,678.25 ± 1584.77	0.74 ± 0.043
Med13/ 13L	+	+	F	4	16.68 ± 0.54	11.25 ± 1.10	187.92 ± 19.44	0.60 ± 0.041	617.5 ± 138.77	17.044 ± 0.99	15.25 ± 0.67	7.98 ± 0.21	7.46 ± 0.23	26.65 ± 0.98	8.54 ± 0.28	113.80 ± 9.37	95.17 ± 6.95	79.97 ± 6.22	1.45 ± 0.16	18.63 ± 4.57	11,382.39 ± 4231.035	0.15 ± 0.037
Med13/ 13L	−	+	F	2	16.73 ± 0.58	6.66 ± 0.29	111.35 ± 1.05	0.80 ± 0.091	728 ± 8	4.37 ± 0.16	0.91 ± 0.02	5.85 ± 0.037	3.77 ± 0.42	14.11 ± 0.23	6.97 ± 0.11	21.33 ± 0.67	2.87 ± 0.38	63.71 ± 0.71	0.33 ± 0.014	18.45 ± 1.059	13,427.51 ± 623.049	0.86 ± 0.022
Med13L	+	+	M	7	29.26 ± 1.21	4.62 ± 0.16	134.41 ± 4.34	0.70 ± 0.029	709.66 ± 10.39	6.81 ± 0.49	1.84 ± 0.22	6.87 ± 0.096	5.85 ± 0.12	17.50 ± 0.79	7.95 ± 0.099	39 ± 2.87	9.021 ± 1.12	80.79 ± 2.63	0.48 ± 0.022	29.97 ± 2.19	21,229.29 ± 1460.28	0.77 ± 0.02
Med13L	−	+	M	7	29.69 ± 1.51	4.53 ± 0.17	133.8 ± 5.68	0.68 ± 0.024	708.5 ± 10.13	6.91 ± 0.51	1.83 ± 0.23	6.79 ± 0.11	5.72 ± 0.13	17.87 ± 0.78	7.84 ± 0.11	39.059 ± 2.92	8.78 ± 1.18	81.52 ± 2.53	0.47 ± 0.024	30.27 ± 2.25	21,412.57 ± 1533.012	0.77 ± 0.022
Med13	+	+	M	6	35.55 ± 1.70	3.84 ± 0.087	136.36 ± 5.68	0.69 ± 0.028	718.55 ± 5.16	6.57 ± 0.34	1.51 ± 0.17	6.73 ± 0.085	5.604 ± 0.12	17.57 ± 0.87	7.85 ± 0.10	36.88 ± 2.086	6.99 ± 0.70	82.19 ± 5.013	0.45 ± 0.01	29.88 ± 2.16	21,467.28 ± 1524.38	0.80 ± 0.022
Med13	−	+	M	4	34.99 ± 2.48	3.96 ± 0.18	137.38 ± 6.40	0.73 ± 0.041	720.77 ± 7.097	6.39 ± 0.49	1.44 ± 0.21	6.85 ± 0.15	5.59 ± 0.15	17.24 ± 1.16	7.97 ± 0.15	36.44 ± 2.72	6.68 ± 0.85	82.08 ± 6.15	0.44 ± 0.015	29.76 ± 2.69	21,434.86 ± 1878.79	0.81 ± 0.026
WT	+	+	M	3	28.3 ± 1.73	4.87 ± 0.50	136.2 ± 6.10	0.75 ± 0.033	687.33 ± 26.86	6.071 ± 0.74	1.30 ± 0.14	7.47 ± 0.15	6.32 ± 0.16	15.94 ± 0.87	8.58 ± 0.17	37.82 ± 4.64	6.90 ± 0.91	80.23 ± 3.15	0.46 ± 0.041	30.92 ± 3.76	21,072.88 ± 1903.47	0.81 ± 0.005
WT	−	+	M	3	28.63 ± 1.84	4.75 ± 0.41	134.41 ± 5.24	0.71 ± 0.033	700.66 ± 19.81	6.17 ± 0.58	1.28 ± 0.19	7.18 ± 0.21	5.83 ± 0.34	16.086 ± 1.076	8.22 ± 0.25	36.92 ± 3.50	6.23 ± 0.99	76.93 ± 4.70	0.47 ± 0.027	30.68 ± 2.89	21,385.62 ± 1586.33	0.83 ± 0.019

26) and Med13/13L fl/fl ($n = 6$). Median survival time for the Med13/13L dKO mice was 6 weeks from start of tamoxifen treatment with 100 % mortality at 10 weeks (Fig. 1D). Med13/13L fl/fl mice survived the time course. This indicates that cardiac Med13/13L plays a critical role in survival.

3.2. Deletion of Med13 and Med13L induces cardiac dysfunction consistent with heart failure

To further investigate the redundant role of Med13/13L, we performed echocardiography on Med13/13L dKO and littermate control mice at 12 weeks of age (Fig. 1E). Echocardiography revealed a significant decrease (~50 %) in ejection fraction between Med13/13L dKO and Med13/13L fl/fl mice in both male and female cohorts (Fig. 2A, Table 1 respectively). There is no difference in heart rate between Med13/13L dKO and Med13/13L fl/fl cohorts (Fig. 2B). There are significant increases in the Heart Weight:Body Weight ratio (~2.9 mg:g increase) and volume/mass (~0.68 μL/mg increase) denoting an enlarged heart (Fig. 2C, D). There are also significant increases in end diastolic volume (~69 μL increase) and end systolic volume (~66 μL increase; (Fig. 2E, F). As expected, there are no significant echocardiographic differences between the single Med13 cKO or Med13L cKO mice, indicating a compensatory mechanism at basal cardiac function (Table 1). WT C57BL/6-MCM males also display no cardiac changes regardless of diet (Table 1). This data indicates that changes seen between Med13/13L dKO and Med13/13L fl/fl cohorts are due to genetic deletion rather than the effect of tamoxifen. Histological analysis using H&E staining showed no significant structural abnormalities in the hearts of Med13/13L dKO mice (Fig. 2G). Overall, these findings indicate that deletion of Med13/13L leads to dilated cardiomyopathy and Med13/13L plays a crucial role in maintaining basal cardiac function.

3.3. Loss of Med13/13L alters gene expression for cardiac fibrosis and excitation-contraction coupling

To determine potential effects of Med13 and Med13L on gene expression, we performed bulk RNA-seq on mouse hearts four weeks after the start of tamoxifen to identify changes in gene expression prior to the development of heart failure. RNA-seq results showed a total of 1062 differentially expressed genes (540 upregulated, 522

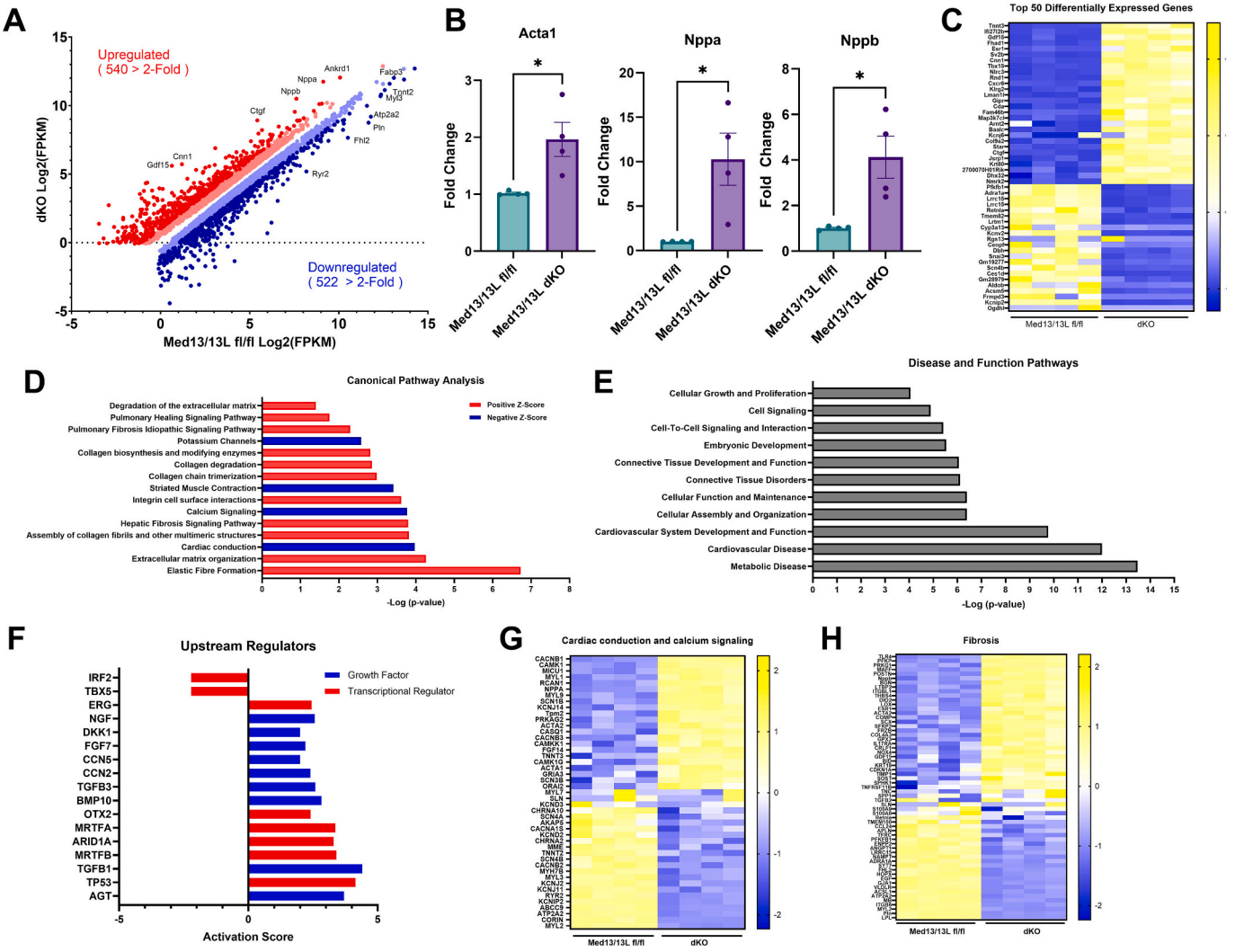

Fig. 3. RNA-seq analysis of Med13/13L dKO mice. A) Dot plot displaying significant genes (Padj <0.05) in muted color and significant/Log2(FC) >1.0 in dark colors. B) Validation of RNAseq hits with qRT-PCR for Acta1, Nppa, and Nppb. (n = 4, performed in triplicate) Unpaired t-test performed with significance classified as $p < 0.05$. C) Heatmap of the top 50 differentially expressed genes. Color code corresponds to z-score. D) Canonical pathways as analyzed by IPA. E) Disease and function pathways as analyzed by IPA. F) Dysregulation of upstream regulators as identified by IPA. G) Heatmap of cardiac conduction and calcium signaling-related genes as indicated by IPA. Color code corresponds to z-score of FPKM values. H) Heatmap of fibrosis-related genes as indicated by IPA. Color code corresponds to z-score of FPKM values.

downregulated, Log2FoldChange >1, q-value <0.05; Fig. 3A). We performed qRT-PCR on Acta1, Nppa, and Nppb to validate our RNAseq results (Fig. 3B) The top 50 differentially expressed genes showcase a consistent expression profile across samples and highlight significant upregulation of genes associated with fibrosis as well as a downregulation of key ion channels (Fig. 3C).

To predict the most likely altered pathways, we applied an expression threshold of Log2FoldChange >1. Ingenuity Pathway Analysis (IPA) of these 540 upregulated and 522 downregulated genes revealed likely upregulated fibrotic and extracellular matrix pathways, as well as a decrease in cardiac excitation-contraction coupling pathways (Fig. 3D). IPA of disease and function pathways showed changes in connective tissues as well as cardiovascular diseases (Fig. 3E). Previous work has associated Med13 and Med13L with embryonic development and metabolic diseases which are also seen in our disease and function pathway analysis highlighting the reproducibility of Med13/13L studies (Fig. 3E) [12,19].

Next, we looked at upstream regulators associated with our bulk RNA-seq dataset through IPA. We found increases in activation in growth factors, such as TGFB1 and TGFB3, which have been previously associated with increases in cardiac fibrosis and had upregulated expression levels (Fig. 3F). Increased activation within key cardiac transcriptional regulators like MRTFA and MRTFB were also noted in the IPA analysis. The associations between the activated upstream regulators with fibrosis and hypertrophy indicate that Med13/13L play a role in modulating the canonical transcriptional responses during cardiac stress. We noted clear differential expression between control and Med13/13L dKO groups for pathways associated with cardiac excitation/contraction coupling (Fig. 3G). Differentially expressed genes associated with cardiac conduction and calcium signaling displayed prominent differences between groups and indicated that key calcium channel genes such as Serca2a, Phospholamban, and RyR2 are affected. Canonical pathway analysis also indicated the upregulation of cardiac fibrosis could be affected by Med13/13L deletion (Fig. 3H).

Due to the upregulation of fibrotic pathways, we investigated the extent of fibrosis in our mice. We performed masson's trichrome staining and quantified the percent area of fibrosis (Fig. 4A). We found a significant increase in stained collagen in our Med13/13L dKO compared to the Med13/13L fl/fl mice (Fig. 4B). We also performed qRT-PCR to validate our RNA-seq results finding a significant increase in col1a1, col3a1, TGFB1 (Fig. 4C–E). These results indicate that the deletion of Med13/13L results in the upregulation and development of fibrosis.

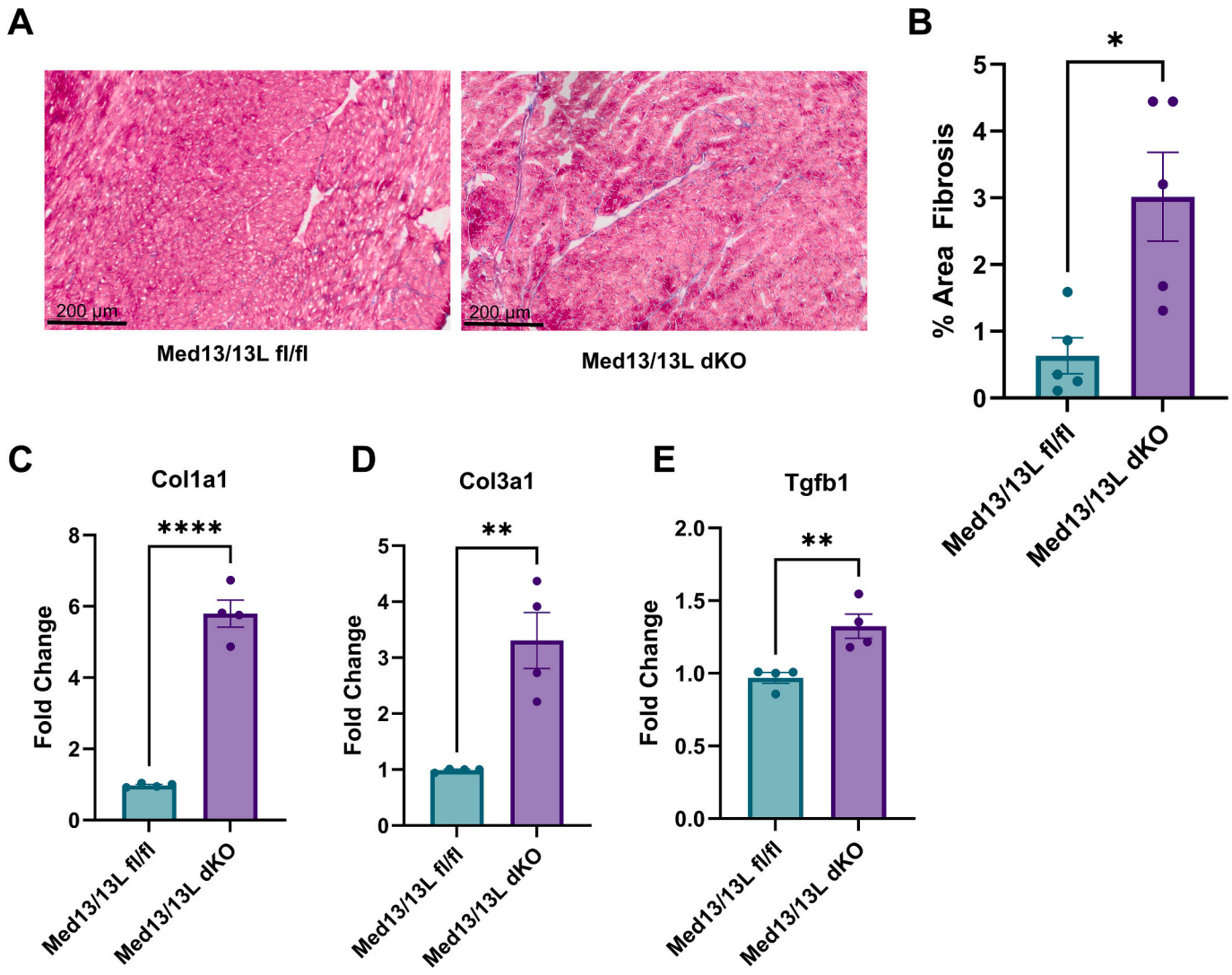

Fig. 4. Med13/13L dKO mice develop cardiac fibrosis. A) Representative images of Mason's trichrome from Med13/13L fl/fl and Med13/13L dKO. B) Quantification of Mason's trichrome. (3 sections imaged per heart, n = 5). C–E) qRT-PCR performed for Col1a1, Col3a1, and Tgfb1 (n = 4, performed in triplicate). All data is displayed with SEM. Unpaired t-test performed with significance classified as $p < 0.05$.

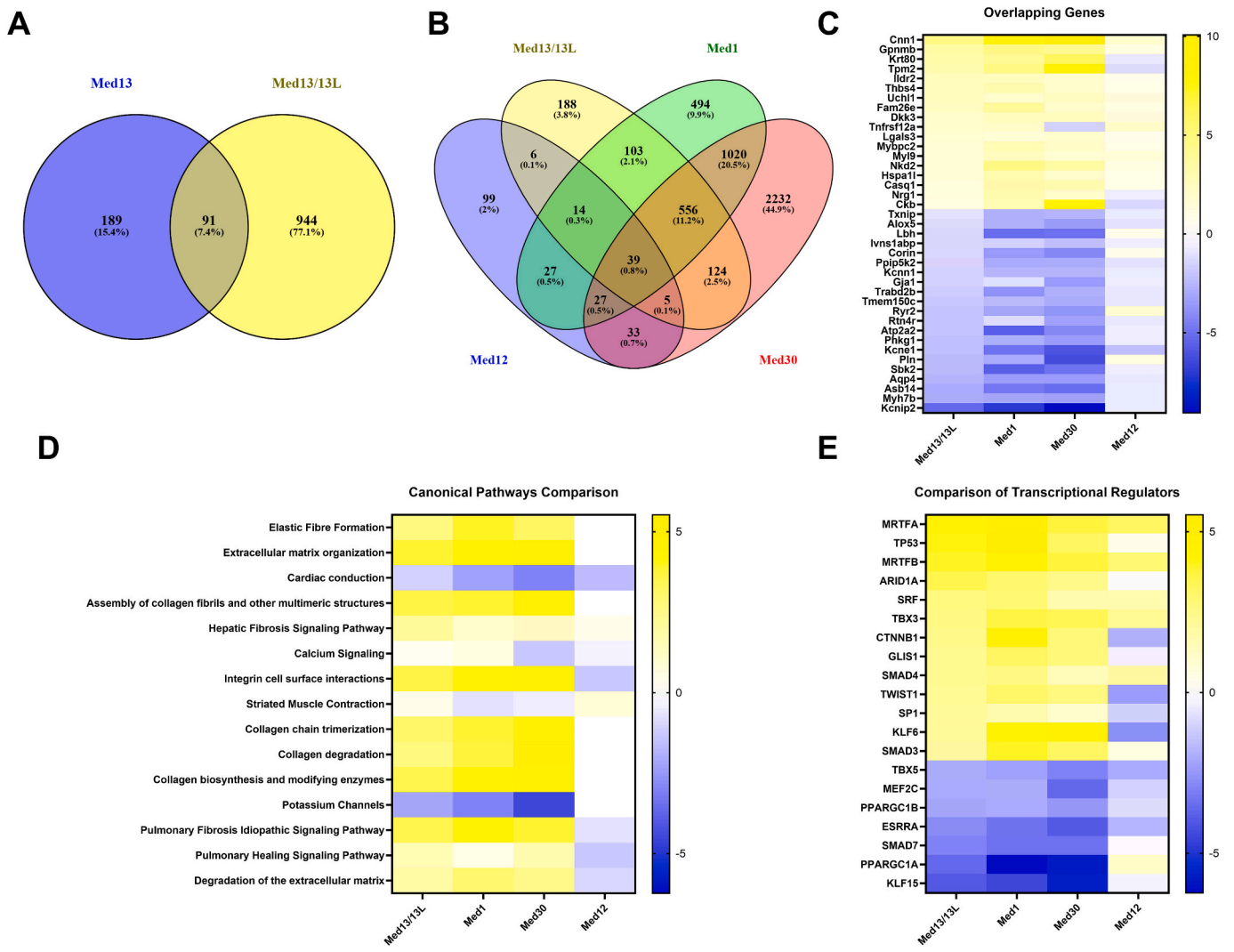

Fig. 5. Comparison of cardiac Mediator deletion phenotypes. A) Overlapping differentially regulated genes from MED13/13L dKO and MED13 cKO mice. B) Overlapping differentially regulated genes from MED13/13L dKO, MED1 cKO, MED30 cKO, and MED12 cKO mice. C) Heatmap of overlapping differentially regulated genes. Color code corresponds to Log2FC. D) Comparison of canonical pathways. Color code corresponds to activation z-score as generated by IPA. E) Comparison of transcriptional regulators. Color code corresponds to activation z-score as generated by IPA.

3.4. Cardiac Mediator deletions result in similar differential gene expression profiles

Cardiac-specific deletion of Med13 alone has been previously reported [18]. We investigated the overlap of differential gene expression between Med13 cKO and Med13/13L dKO mice. We used the same differential gene expression thresholds as previously stated in Minerath et al. [18]. However, there were only 91 overlapping genes between these data sets, accounting for only 7.9 % of the total genes dysregulated amongst the two datasets (Fig. 5A). The lethality associated with the Med13/13L dKO and the dysregulated genes not seen in Med13 cKO indicate that these genes work primarily redundantly in the heart. However, there is independent gene dysregulation in the Med13 cKO and within the overlap displaying that there could be independent roles for Med13 and Med13L.

Previous work has characterized other Mediator subunits within the heart which have overlapping cardiac phenotypes, such as dilated cardiomyopathy, early lethality, and decreased cardiac excitation/contractin coupling [18,25,27,28]. We compared overlapping differentially expressed genes from cardiac Med1 conditional knockouts at 3 weeks, inducible Med30 cardiomyocyte specific knockout at 4 weeks post-tamoxifen, and cardiomyocyte-specific Med12 knockout at postnatal day 1 (P1), alongside our Med13/13L cardiomyocyte-specific knockouts [25,27,28]. We used the same thresholds to calculate differential gene expressions as performed by the original investigators and compared for overlapping differentially regulated gene networks. We found 39 total genes differentially expressed between all four Mediator cardiac knockouts (Fig. 5B). Of these 39 genes, most had similar upregulation/downregulation as the Med13/13L dKO (Fig. 5C). We performed a comparative IPA analysis on the different RNA-seq datasets to identify similarities in downstream targets by examining IPA-generated activation z-scores for canonical pathways identified previously (Fig. 5D). We saw a similar downregulation across the four different datasets for cardiac conduction. Med13/13L, Med1, and Med30 shared similar pathway analysis for different fibrosis pathways as well as downregulation of potassium channels. We next examined the comparison of transcriptional regulators using a threshold of activation z-score above 2 for Med13/13L and found 20 transcriptional regulators affected in all four datasets with similar differential expression patterns between the Med13/13L, Med1, and Med30 datasets (Fig. 5E). Overall, the mediator complex acts as a critical driver for basal cardiac function, in which all four mediator knockouts develop similar dysregulation of cardiac gene networks.

4. Discussion

Maintenance of cardiac function requires coordinated gene expression. The Mediator complex functions to integrate cell signaling events with RNA polymerase II-dependent transcription. However, few studies have determined the functional role of individual subunits, or the redundant function of Mediator subunit homologs such as Med13 and Med13L. We generated double knockouts of Med13/13L to test the role of Med13/13L in adult cardiomyocyte homeostasis. Our study demonstrates that Med13 and Med13L function partially redundantly to maintain basal cardiac function. In line with previous literature demonstrating functional redundancy in embryo development and super-enhancer utilization, we determined that Med13 and Med13L single deletions can maintain basal cardiac function, whereas a double deletion of Med13/13L is lethal within an average time frame of 6 weeks [11,12]. This is consistent with other Mediator complex subunits, in which there are some compensatory mechanisms at play in development, but under stress cannot maintain basal function [18,25,33]. While our study displayed redundancy in maintaining basal cardiac function, future studies should investigate independent compensatory mechanisms to determine differences in single Mediator gene deletions in cardiac stress responses.

Analysis of upstream regulators coincided with previously known fibrotic pathways. TBX5 was downregulated in Med13/13L dKO samples and has been shown to regulate cardiac conduction and play a role in cardiac maturation [34]. Growth factors such as CCN2, TGFB1 and TGFB3 were all upregulated. TGFB1 is an essential factor in inducing cardiac fibrosis and has been noted in models of dilated, ischemic, and hypertrophic cardiomyopathies, as well as valvular diseases and arrythmias [35]. TGFB3 is a less understood isoform of the TGF family yet has been implicated in fibrotic disease pathogenesis [36]. CCN2 acts as an autocrine factor in the heart to induce cardiac fibrosis [37]. Transcriptional regulators have also been highlighted, including MRTFa/b, responsible for controlling fibrotic gene programs and myofibroblast activation [38,39]. Overall, the cumulative result is that a lack of Med13/13L results in a transcriptional shift toward fibrotic pathways.

Fibrosis can play a large role in the development of heart failure [40–42]. Within the fibrotic pathways, increased expression in fibrotic proteins such as POSTN and BGN are known to upregulate cardiac fibrosis [43,44]. It is interesting to note such a large differential expression of fibroblast specific genes since our study specifically deleted Med13/13L in cardiomyocytes. This indicates possible cardiomyocyte-to-fibroblast crosstalk. We also noted changes in expression of calcium and potassium channels, another possible mechanism driving heart failure in Med13/13L cardiac deletions. Calcium channels such as Serca2a, PLN, and Ryr2 have been previously shown to play a role in the induction of heart failure [45–48]. The downregulation of these channels in Med13/13L dKO mice indicates possible impaired cardiac excitation/contraction coupling, which can lead to reduced cardiac contraction and ultimately, heart failure.

The 91 overlapping genes between Med13 and Med13/13L cardiac knockouts could signal that these genes may be regulated through the dose response of Med13/13L or in a Med13-independent manner. We also see 944 genes only differentially regulated in Med13/13L dKO, which could highlight the redundant function of Med13/13L since they were only affected after deletion of Med13L and are associated with cardiac lethality. A limitation to this comparison is that the datasets were generated under different timepoints and Cre drivers therefore they are two distinct model systems. However, the underlying overlap still displays both redundant and independent Med13 functions as expected. Cardiac Mediator knockouts of Med1, Med12, Med30 and now Med13/13L all display similar phenotypes in which deletion of the respective subunit results in gene dysregulation and dilated cardiomyopathy [25,27,28]. Despite the differences in time points for RNA-seq, there is substantial overlap of gene expression changes between the four groups, indicating that there could be conserved mechanisms across the Mediator complex which regulate basal cardiac function. The differences associated with Med12 could be due to the early postnatal timepoint compared to the other datasets at adult stages. The conserved genes across the four groups include calcium handling genes such as Serca2a, Pln, and Ryr2 as well as heart failure markers such as Myh7b. This suggests redundancy not only in Med13/13L, but also within the Mediator complex kinase submodule, as basal cardiac function relies on a functional mediator complex.

Overall, our work demonstrated the redundant nature of Med13/13L in preserving basal cardiac function as well as relating the cardiac phenotype to other Mediator cardiac phenotypes in which similar gene dysregulation occurs. The early lethality associated with Med13/13L dKO mice renders difficulties in studying the mechanisms causing heart failure with a particular limitation in determining if gene expression changes are direct consequences of Med13/13L deletion or secondary to heart failure. However, we can infer the mode in which lethality occurs through previous Mediator studies. Future work should begin elucidating the independent roles of Med13 and Med13L in the heart, as well as differences in how the single knockouts respond to cardiac stress.

CRediT authorship contribution statement

Kayla M. Henry: Writing – review & editing, Writing – original draft, Validation, Investigation, Formal analysis, Data curation. **Richard N. Gardner:** Writing – review & editing, Investigation, Formal analysis. **Alexis M. Oppman:** Investigation. **Nastaran Daneshgar:** Investigation. **Mariela Rosales:** Investigation. **Ines Martins:** Investigation. **Kedryn K. Baskin:** Writing – review & editing, Writing – original draft, Formal analysis. **Chad E. Grueter:** Writing – review & editing, Resources, Project administration, Methodology, Funding acquisition, Formal analysis, Conceptualization.

Sources of funding

This work was funded by the NIH/NHLBI 1 R01HL168044 (CEG), NIH Predoctoral Training Grant T32GM145441 (KMH), the MED13L Foundation, and R01HL166520 (KKB).

Declaration of competing interest

The authors declare that they have no known competing financial interests or personal relationships that could have appeared to influence the work reported in this paper.

Acknowledgements

The Genomics Division of the Iowa Institute on Human Genetics generated the RNA sequencing library and data through the support of the University of Iowa Institute on Human genetics which is supported, in part, by the University of Iowa Carver College of Medicine. Echocardiography services were performed by the University of Iowa Cardiovascular Imaging Core using the Vevo 2100 system which was purchased using NIH grants S10 OD019941-01 and S10 RR026293-01. Histology was performed at the University of Iowa Central Microscopy Research Facility, which is supported by the Vice President for Research & economic development, the Holden Comprehensive Cancer Center, and the Carver College of Medicine. Histology was performed at the University of Iowa Pathology Core.

References

[1] Kathiriya IS, Nora EP, Bruneau BG. Investigating the transcriptional control of cardiovascular development. Circ Res 2015;116(4):700–14.
[2] Sunny S, Challa AK, Qiao A, Jyothidasan A, Krishnamurthy P, Ramamurthy MT, et al. Transcriptional regulation of structural and functional adaptations in a developing adulthood myocardium. Cardiol Cardiovasc Med 2021;5(5):454–70.

[3] Koenig AL, Shchukina I, Amrute J, Andhey PS, Zaitsev K, Lai L, et al. Single-cell transcriptomics reveals cell-type-specific diversification in human heart failure. Nat Cardiovasc Res 2022;1(3):263–80.
[4] de Carvalho A, Cordeiro MA, Rodrigues LS, Ortolani D, Spadari RC. Stress-induced differential gene expression in cardiac tissue. Sci Rep 2021;11(1):9129.
[5] Richter WF, Nayak S, Iwasa J, Taatjes DJ. The mediator complex as a master regulator of transcription by RNA polymerase II. Nat Rev Mol Cell Biol 2022;23(11):732–49.
[6] Akazawa H, Komuro I. Roles of cardiac transcription factors in cardiac hypertrophy. Circ Res 2003;92(10):1079–88.
[7] Vigil-Garcia M, Demkes CJ, Eding JEC, Versteeg D, de Ruiter H, Perini I, et al. Gene expression profiling of hypertrophic cardiomyocytes identifies new players in pathological remodelling. Cardiovasc Res 2021;117(6):1532–45.
[8] Conaway RC, Sato S, Tomomori-Sato C, Yao T, Conaway JW. The mammalian mediator complex and its role in transcriptional regulation. Trends Biochem Sci 2005;30(5):250–5.
[9] Bourbon HM. Comparative genomics supports a deep evolutionary origin for the large, four-module transcriptional mediator complex. Nucleic Acids Res 2008;36(12):3993–4008.
[10] Muncke N, Jung C, Rudiger H, Ulmer H, Roeth R, Hubert A, et al. Missense mutations and gene interruption in PROSIT240, a novel TRAP240-like gene, in patients with congenital heart defect (transposition of the great arteries). Circulation 2003;108(23):2843–50.
[11] Kuuluvainen E, Domenech-Moreno E, Niemela EH, Makela TP. Depletion of mediator kinase module subunits represses superenhancer-associated genes in colon cancer cells. Mol Cell Biol 2018;38(11).
[12] Miao YL, Gambini A, Zhang Y, Padilla-Banks E, Jefferson WN, Bernhardt ML, et al. Mediator complex component MED13 regulates zygotic genome activation and is required for postimplantation development in the mouse. Biol Reprod 2018;98(4):449–64.
[13] Asadollahi R, Oneda B, Sheth F, Azzarello-Burri S, Baldinger R, Joset P, et al. Dosage changes of MED13L further delineate its role in congenital heart defects and intellectual disability. Eur J Hum Genet 2013;21(10):1100–4.
[14] Borik S, Simon AJ, Nevo-Caspi Y, Mishali D, Amariglio N, Rechavi G, et al. Increased RNA editing in children with cyanotic congenital heart disease. Intensive Care Med 2011;37(10):1664–71.
[15] Napoli C, Schiano C, Soricelli A. Increasing evidence of pathogenic role of the mediator (MED) complex in the development of cardiovascular diseases. Biochimie 2019;165:1–8.
[16] Trivisano M, De Dominicis A, Micalizzi A, Ferretti A, Dentici ML, Terracciano A, et al. MED13 mutation: a novel cause of developmental and epileptic encephalopathy with infantile spasms. Seizure 2022;101:211–7.
[17] Utami KH, Winata CL, Hillmer AM, Aksoy I, Long HT, Liany H, et al. Impaired development of neural-crest cell-derived organs and intellectual disability caused by MED13L haploinsufficiency. Hum Mutat 2014;35(11):1311–20.
[18] Minerath RA, Dewey CM, Hall DD, Grueter CE. Regulation of cardiac transcription by thyroid hormone and Med13. J Mol Cell Cardiol 2019;129:27–38.
[19] Grueter CE, van Rooij E, Johnson BA, DeLeon SM, Sutherland LB, Qi X, et al. A cardiac microRNA governs systemic energy homeostasis by regulation of MED13. Cell 2012;149(3):671–83.
[20] Baskin KK, Grueter CE, Kusminski CM, Holland WL, Bookout AL, Satapati S, et al. MED13-dependent signaling from the heart confers leanness by enhancing metabolism in adipose tissue and liver. EMBO Mol Med 2014;6(12):1610–21.
[21] Baskin KK, Winders BR, Olson EN. Muscle as a "mediator" of systemic metabolism. Cell Metab 2015;21(2):237–48.
[22] Chang KT, Jezek J, Campbell AN, Stieg DC, Kiss ZA, Kemper K, et al. Aberrant cyclin C nuclear release induces mitochondrial fragmentation and dysfunction in MED13L syndrome fibroblasts. iScience 2022;25(2):103823.
[23] Jia Y, Chang HC, Schipma MJ, Liu J, Shete V, Liu N, et al. Cardiomyocyte-specific ablation of Med1 subunit of the mediator complex causes lethal dilated cardiomyopathy in mice. PloS One 2016;11(8):e0160755.
[24] Ponce JM, Coen G, Spitler KM, Dragisic N, Martins I, Hinton Jr A, et al. Stress-induced cyclin C translocation regulates cardiac mitochondrial dynamics. J Am Heart Assoc 2020;9(7):e014366.
[25] Spitler KM, Ponce JM, Oudit GY, Hall DD, Grueter CE. Cardiac Med1 deletion promotes early lethality, cardiac remodeling, and transcriptional reprogramming. Am J Physiol Heart Circ Physiol 2017;312(4):H768–80.
[26] Hall DD, Ponce JM, Chen B, Spitler KM, Alexia A, Oudit GY, et al. Ectopic expression of Cdk8 induces eccentric hypertrophy and heart failure. JCI Insight 2017;2(15).
[27] Baskin KK, Makarewich CA, DeLeon SM, Ye W, Chen B, Beetz N, et al. MED12 regulates a transcriptional network of calcium-handling genes in the heart. JCI Insight 2017;2(14).
[28] Tan C, Zhu S, Chen Z, Liu C, Li YE, Zhu M, et al. Mediator complex proximal tail subunit MED30 is critical for mediator core stability and cardiomyocyte transcriptional network. PLoS Genet 2021;17(9):e1009785.
[29] Zhu S, Chen Z, Liu C, Duong J, Tran T, Liang Z, et al. The essential role of MED27 in stabilizing the mediator complex for cardiac development and function. Life Sci 2024;356:123020.
[30] Skarnes WC, Rosen B, West AP, Koutsourakis M, Bushell W, Iyer V, et al. A conditional knockout resource for the genome-wide study of mouse gene function. Nature 2011;474(7351):337–42.
[31] Oliveros JC. Venny. An interactive tool for comparing lists with Venn's diagrams. https://bioinfogp.cnb.csic.es/tools/venny/index.html; 2007-2015.
[32] Simossis VA, Heringa J. PRALINE: a multiple sequence alignment toolbox that integrates homology-extended and secondary structure information. Nucleic Acids Res 2005;33(Web Server issue):W289–94.
[33] Hall DD, Spitler KM, Grueter CE. Disruption of cardiac Med1 inhibits RNA polymerase II promoter occupancy and promotes chromatin remodeling. Am J Physiol Heart Circ Physiol 2019;316(2):H314–25.
[34] Steimle JD, Moskowitz IP. TBX5: a key regulator of heart development. Curr Top Dev Biol 2017;122:195–221.
[35] Khan R, Sheppard R. Fibrosis in heart disease: understanding the role of transforming growth factor-beta in cardiomyopathy, valvular disease and arrhythmia. Immunology 2006;118(1):10–24.
[36] Sun T, Huang Z, Liang WC, Yin J, Lin WY, Wu J, et al. TGFbeta2 and TGFbeta3 isoforms drive fibrotic disease pathogenesis. Sci Transl Med 2021;13(605).
[37] Dorn LE, Petrosino JM, Wright P, Accornero F. CTGF/CCN2 is an autocrine regulator of cardiac fibrosis. J Mol Cell Cardiol 2018;121:205–11.
[38] Small EM, Thatcher JE, Sutherland LB, Kinoshita H, Gerard RD, Richardson JA, et al. Myocardin-related transcription factor-a controls myofibroblast activation and fibrosis in response to myocardial infarction. Circ Res 2010;107(2):294–304.
[39] Mokalled MH, Carroll KJ, Cenik BK, Chen B, Liu N, Olson EN, et al. Myocardin-related transcription factors are required for cardiac development and function. Dev Biol 2015;406(2):109–16.
[40] Rockey DC, Bell PD, Hill JA. Fibrosis–a common pathway to organ injury and failure. N Engl J Med 2015;372(12):1138–49.
[41] Baudino TA, Carver W, Giles W, Borg TK. Cardiac fibroblasts: friend or foe? Am J Physiol Heart Circ Physiol 2006;291(3):H1015–26.
[42] Travers JG, Kamal FA, Robbins J, Yutzey KE, Blaxall BC. Cardiac fibrosis: the fibroblast awakens. Circ Res 2016;118(6):1021–40.
[43] Gil H, Goldshtein M, Etzion S, Elyagon S, Hadad U, Etzion Y, et al. Defining the timeline of periostin upregulation in cardiac fibrosis following acute myocardial infarction in mice. Sci Rep 2022;12(1):21863.
[44] Scuruchi M, Mannino F, Imbesi C, Pallio G, Vermiglio G, Bagnato G, et al. Biglycan involvement in heart fibrosis: modulation of sdenosine 2A receptor improves damage in immortalized cardiac fibroblasts. Int J Mol Sci 2023;24(2).
[45] Li L, Louch WE, Niederer SA, Aronsen JM, Christensen G, Sejersted OM, et al. Sodium accumulation in SERCA knockout-induced heart failure. Biophys J 2012;102(9):2039–48.
[46] Bround MJ, Asghari P, Wambolt RB, Bohunek L, Smits C, Philit M, et al. Cardiac ryanodine receptors control heart rate and rhythmicity in adult mice. Cardiovasc Res 2012;96(3):372–80.
[47] Jiang Y, Li X, Guo T, Lu WJ, Ma S, Chang Y, et al. Ranolazine rescues the heart failure phenotype of PLN-deficient human pluripotent stem cell-derived cardiomyocytes. Stem Cell Reports 2022;17(4):804–19.
[48] Marks AR. Calcium cycling proteins and heart failure: mechanisms and therapeutics. J Clin Invest 2013;123(1):46–52.